

## Application of the three-body model to the reactions ${}^6\text{Li}({}^3\text{He}, t\ {}^3\text{He}){}^3\text{He}$ and ${}^6\text{Li}({}^3\text{He}, {}^3\text{He}{}^3\text{He}){}^3\text{H}$

M. I. Haftel, R. G. Allas, L. A. Beach, R. O. Bondelid, and E. L. Petersen  
*Naval Research Laboratory, Washington, D. C. 20375*

Ivo Šlaus

*Institute Ruder Bosković, Zagreb, Yugoslavia  
 and Naval Research Laboratory, Washington, D. C. 20375*

J. M. Lambert and P. A. Treado

*Georgetown University, Washington, D. C. 20007  
 and Naval Research Laboratory, Washington, D. C. 20375*

(Received 11 March 1977)

Experimental and theoretical cross sections are presented for the  ${}^6\text{Li}({}^3\text{He}, {}^3\text{He}{}^3\text{He}){}^3\text{H}$  and  ${}^6\text{Li}({}^3\text{He}, t\ {}^3\text{He}){}^3\text{He}$  reactions for the symmetric angle pairs  $20^\circ$ - $20^\circ$ ,  $28.3^\circ$ - $28.3^\circ$ , and  $35^\circ$ - $35^\circ$ . The theoretical cross sections are calculated in a three-body model where the trions (i.e., mass-3 nuclei) are treated as elementary particles with  ${}^6\text{Li}$  being a  ${}^3\text{He}$ - ${}^3\text{H}$  bound state. The trion-trion interaction is represented by  $S$  wave separable potentials with the breakup cross sections calculated with the three-body Haftel-Ebenhöh code. The Coulomb interaction is taken into account by fitting the separable potential parameters to the trion-trion scattering data and is included approximately in the breakup code. The experimental cross sections are compared with both the plane-wave impulse approximation and the three-body model predictions. The plane-wave impulse approximation predicts both the shapes and magnitudes poorly (10 to 20 times experiment). Without Coulomb corrections the three-body model gives good agreement with experiment for the shapes of the spectra with the magnitudes generally being about 40% of experiment for  ${}^6\text{Li}({}^3\text{He}, {}^3\text{He}{}^3\text{He}){}^3\text{H}$  and about 80% for  ${}^6\text{Li}({}^3\text{He}, t\ {}^3\text{He}){}^3\text{He}$ . The Coulomb corrections improve the magnitudes predicted by the three-body model but not the shapes. It is observed that for these reactions  $S$  wave separable potentials describe the breakup data much better than they do the two-body trion-trion scattering data. This result should encourage further three-body treatment of these and similar reactions.

[NUCLEAR REACTIONS  ${}^6\text{Li}({}^3\text{He}, {}^3\text{He}{}^3\text{He}){}^3\text{H}$ ,  ${}^6\text{Li}({}^3\text{He}, t\ {}^3\text{He}){}^3\text{He}$ ,  $E = 45$  MeV, ]  
 tractable Faddeev calculations  $\sigma(E, \theta_1, \theta_2)$ , Coulomb corrections.

### I. INTRODUCTION

The Faddeev equations have had great success in predicting the experimental properties of the three nucleon system.<sup>1-5</sup> In particular, the three-body treatment of nucleon induced deuteron breakup, pioneered by Amado,<sup>2</sup> has succeeded in predicting experimental cross sections in many regions of phase space with very simple  $N$ - $N$  interactions. In recent years there has been much interest in applying such three-body methods to more complex nuclear reactions.<sup>6-9</sup> Here, of course, one does not have three "elementary" particles as in the  $3N$  case, but perhaps in the particular reactions under consideration<sup>6-9</sup> the particles can be approximated as three "elementary" constituents, e.g.,  $\alpha$  particles and trions (mass-3 nuclei). This approach might be a considerable improvement over plane-wave and distorted-wave theories (PWBA, DWBA, PWIA, and DWIA) which are essentially two-body theories. Approximate three-body theories for deuteron stripping and

pickup have been developed by Soper and Johnson, Rawitscher and others<sup>6</sup>; and the six nucleon system has been treated as a three-body problem: nucleon-nucleon- $\alpha$ .<sup>7</sup> The  ${}^6\text{Li}$  spectrum (and  ${}^6\text{He}$  ground state) and the  $d$ - $\alpha$  elastic scattering cross section and polarization have been predicted reasonably well<sup>7,8</sup> using the nucleon- $\alpha$  ( $s_{1/2}$ ,  $p_{3/2}$ , and  $p_{1/2}$ ) and nucleon-nucleon ( ${}^1S_0$ ,  ${}^3S_1$  +  ${}^3D_1$ ) separable interactions. These calculations are carried out in the framework that the coupling to the  ${}^3\text{He}({}^3\text{H})$ - ${}^3\text{H}$  channel is weak. Chuu, Hau, and Lin<sup>9</sup> have approximately taken into account the internal structure of the  $\alpha$  particle by representing it as a two-state system. Shanley<sup>7</sup> and Charnormodic, Fayard, and Lamot<sup>8</sup> simulate Coulomb effects by adding Coulomb scattering amplitudes to pure nuclear amplitudes. The initial results of these first three-body calculations have been encouraging. Much work on three-body reaction theories<sup>10</sup> has appeared in the literature but has yet to be tested in calculations or experiment.

In the present paper we consider the reactions

${}^6\text{Li}({}^3\text{He}, {}^3\text{He}^3\text{He})^3\text{H}$  and  ${}^6\text{Li}({}^3\text{He}, t^3\text{He})^3\text{He}$  and their theoretical interpretation. Our model<sup>11,12</sup> considers this system as made up of three trions ( ${}^2\text{He}$  and  ${}^3\text{H}$ ). We use both a PWIA calculation and a three-body calculation where the trions are assumed to interact via  $S$  wave separable potentials. These reactions are in many ways analogous to the  ${}^2\text{H}(p, pp)n$  and  ${}^2\text{H}(p, pn)p$  reactions since the mass ratios and the spins are the same. Therefore, the existing Haftel modified Ebenhöf code,<sup>3</sup> with some straightforward modifications, can be used. Since the deuteron breakup reaction has been extensively studied,<sup>4</sup> the comparison with the  ${}^6\text{Li}$  breakup should be of interest.

There are a number of incentives for investigating the theoretical and experimental aspects of the reactions  ${}^6\text{Li}({}^3\text{He}, {}^3\text{He}^3\text{He})^3\text{H}$  and  ${}^6\text{Li}({}^3\text{He}, t^3\text{He})^3\text{He}$ . The  ${}^6\text{Li}+{}^3\text{He}$  reactions have a number of features that differ significantly from the  $p+d$  reactions. It is clear that Coulomb effects can be expected to be substantially more important in the three trion than in the  ${}^2\text{H}(p, pp)n$  reaction. This feature, in fact, has led to an attempt to incorporate a Coulomb interaction term in the computer code used in this analysis in the anticipation of gaining a better understanding of the importance of Coulomb interaction in three-body problems. Another important difference in these systems is exemplified by the trion-trion angular distributions compared with those for the nucleon-nucleon systems. Whereas the nucleon-nucleon interaction below 10 MeV c.m. energy is predominantly  $S$  wave, and even at higher energies one can simulate the almost isotropic angular distributions by an  $S$  wave potential, this is certainly not true for the trion-trion interaction. The trion-trion angular distributions have strong angular and energy dependence. At low energies ( $E_{\text{c.m.}} < 5$  MeV) the anisotropy occurs due to the dominance of the Coulomb interaction and for  $E_{\text{c.m.}} > 5$  MeV higher partial waves become important. The large differences in binding energies can also be expected to play a significant role. The deuteron is bound by just 2.2 MeV, but the two trions in  ${}^6\text{Li}$  are bound by 15.8 MeV. Thus, one expects in the  ${}^6\text{Li}+{}^3\text{He}$  reactions the quasifree scattering (QFS) enhancements to be considerably broader and the short range aspects of the nuclear force to be considerably more important than in the weakly bound system. It should not be overlooked that trions are not fundamental particles, but have their own complex internal structure. Indeed, at all energies nonelastic channels are open for the trion-trion system and consequently the trion-trion interaction should be represented by a complex potential.

Our description of the  ${}^6\text{Li}$  ground state wave function as  ${}^3\text{H}+{}^3\text{He}$  clusters is certainly incom-

plete since other cluster configurations are possible and in particular  ${}^6\text{Li}$  is often described as a bound system of an  $\alpha$  particle and a neutron plus proton<sup>7</sup> or as an  $\alpha$ - $d$  cluster. Plattner *et al.*<sup>13</sup> have determined in a model independent way the  ${}^6\text{Li}$ - $\alpha$ - $d$  coupling constant from the  $\alpha$ - $d$  scattering. They conclude that the overall  $\alpha$ - $d$  cluster probability in  ${}^6\text{Li}$  is between 30 and 60%. This value agrees with those of Jain *et al.*<sup>14</sup> and Noble.<sup>15</sup> The studies of the reaction  ${}^6\text{Li}(\gamma, t)^3\text{He}$  suggest<sup>16</sup> that there is a considerable fraction of the  $t+{}^3\text{He}$  cluster configuration in  ${}^6\text{Li}$ .<sup>17</sup> Evidence for the  $t+{}^3\text{He}$  cluster configuration also comes from the analyses of the reactions  ${}^7\text{Li}({}^3\text{He}, \alpha){}^6\text{Li}$  and  ${}^{11}\text{B}({}^3\text{He}, {}^6\text{Li}){}^8\text{Be}$ .<sup>18</sup> The QFS has been used to study the cluster structure of  ${}^6\text{Li}$ . The measurements of the cross sections for the reactions  ${}^6\text{Li}(\alpha, \alpha x)y$  with  $x=p, d, t, {}^3\text{He}$ , and  $\alpha$  have provided an indication that  ${}^6\text{Li}$  has strong  $p, d$ , and  $\alpha$  clustering, while the  ${}^3\text{H}$ - ${}^3\text{He}$  cluster configuration is considerably weaker.<sup>19</sup> The  ${}^6\text{Li}(p, p^3\text{He})^3\text{H}$  reaction<sup>20</sup> has been investigated at 100 and 156 MeV. It seems that the nucleus  ${}^6\text{Li}$  reveals both  $\alpha$ - $d$  and  ${}^3\text{H}$ - ${}^3\text{He}$  cluster structure. The explanation of this duality has been discussed by Kurdyumov, Neudatchin, and Smirnov<sup>21</sup> and it has been argued that the cluster structures  $\alpha$ - $d$  and  ${}^3\text{H}$ - ${}^3\text{He}$  are not orthogonal, the respective reduced widths  $\theta_t^2$  and  $\theta_d^2$  are both large and  $\theta_t^2 \approx \frac{1}{2}\theta_d^2$ . One hopes that the study of the reactions  ${}^6\text{Li}({}^3\text{He}, {}^3\text{He}^3\text{He})^3\text{H}$  and  ${}^6\text{Li}({}^3\text{He}, t^3\text{He})^3\text{He}$  using three-body models will provide some information on the cluster structure of  ${}^6\text{Li}$ .

The plane-wave impulse approximation has been able to describe the salient features of the deuteron breakup. However, the comparison<sup>22</sup> between the QFS processes  ${}^2\text{H}(p, pp)n$  and  ${}^2\text{H}(p, pn)p$  has demonstrated its inadequacy and the need for the Faddeev approach. Since the spin-isospin structure of  ${}^6\text{Li}+{}^3\text{He}$  is the same as that of  $d+p$ , it is expected that the comparison between  ${}^6\text{Li}({}^3\text{He}, {}^3\text{He}^3\text{He})^3\text{H}$  and  ${}^6\text{Li}({}^3\text{He}, t^3\text{He})^3\text{He}$  in the PWIA and in the Amado model will lead to a better understanding of these reactions.

## II. EXPERIMENTAL APPARATUS AND PROCEDURES

An analyzed 45 MeV helium-3 beam from the Naval Research Laboratory cyclotron was focused on a self-supporting 5.6-mg/cm<sup>2</sup>  ${}^6\text{Li}$  target. Energy correlation data were obtained with the target in a 76-cm scattering chamber. Two silicon surface-barrier detector telescopes and associated electronics, including particle identification and time coincidence event selection, in conjunction with an on-line computer based data acquisition system were used. All charged particle coincidence

events were recorded on magnetic tape and the trion-trion coincident events were selected for on-line monitoring and analysis. The resolving time of the system was approximately 60 nsec. Since the particles of the beam and one or both detected particles were the same, it was necessary to subtract background events for the most forward angle pair used. In all cases the off-line analysis agrees with the on-line results.

The data were obtained at three symmetric angle pairs:  $20^\circ$ - $20^\circ$ ,  $35^\circ$ - $35^\circ$ , and  $28.3^\circ$ - $28.3^\circ$ . The last angle pair was chosen because it contains that portion of phase space for which one of the final state particles has zero momentum in the laboratory system (QFS region). The upper portion of the kinematic locus data was used for analysis; thus, the spectator was in the target. The experimental setup is described in greater detail in a previously published paper.<sup>23</sup>

### III. THEORY

To calculate cross sections for the  ${}^6\text{Li}$ -( ${}^3\text{He}$ ,  ${}^3\text{He}{}^3\text{He}$ ) ${}^3\text{H}$  and  ${}^6\text{Li}$ ( ${}^3\text{He}$ ,  $t$   ${}^3\text{He}$ ) ${}^3\text{He}$  reactions we employ a three-body approach based on the Amado model.<sup>2</sup> With the assumption that  ${}^6\text{Li}$  is constituted of two "elementary" trions (a triton and a  ${}^3\text{He}$ ) we solve the three-body Faddeev equations for breakup with the two-body force being a trion-trion  $S$ -wave real separable potential. The potential chosen predicts the correct  ${}^6\text{Li}$  binding energy as well as the energy of the lowest lying state ( $0^+$  resonance) in  ${}^6\text{Be}$ . For simplicity the nuclear interaction is taken to be charge-independent which seems justified due to the closeness of the experimental binding energies of the lowest lying  $0^+$  states in  ${}^6\text{Be}$  and  ${}^6\text{Li}$  (11.49 and 12.23 MeV below their respective two-trion thresholds). In addition to employing bound state energies, we also used the low-energy experimental  ${}^3\text{He}$ - ${}^3\text{H}$  and  ${}^3\text{He}$ - ${}^3\text{He}$  scattering data in determining potential parameters. The criterion for fits to the two-body data will be discussed shortly. Once the potentials are chosen, they provide the basic input for the three-body—a slightly modified version of the Haftel-Ebenhöh code<sup>3,5</sup>—to calculate  ${}^6\text{Li}$  breakup amplitudes and cross sections.

The main advantage in our calculational technique is that it provides an extremely close parallel to the already widely used separable potential codes used in the three-nucleon ( $3N$ ) problem. As in the deuteron breakup reaction there are three identical spin  $\frac{1}{2}$  fermions with the target being a spin  $1^+$  quasi-two-body bound state. As in the  $3N$  problem, the two-body short-range interaction at low energies is taken to be  $S$  wave. Moreover, only minor modifications of the existing  $3N$  Haftel-Ebenhöh

code (changes in two-body binding energy and changes in the single particle masses) are necessary to apply it to trion induced  ${}^6\text{Li}$  breakup. Our calculations represent the first attempt to study three-body effects exactly in this reaction albeit with an oversimplified model of the interaction and of the ground state of  ${}^6\text{Li}$ . The possible limitations to our approach are numerous. Trions are not elementary particles; therefore, because of inelasticities present in trion-trion scattering, a complex potential is more appropriate than a real potential. Also, the trion-trion cross sections are much less isotropic than corresponding  $N$ - $N$  cross sections. At low energies ( $E_{\text{lab}} < 10$  MeV) the anisotropy occurs due to the dominance of the Coulomb interaction and, for  $E_{\text{lab}} > 10$  MeV, higher partial waves become important. These two factors, which tend to decrease the validity of an  $S$ -wave treatment, are more important than in the previously studied nucleon induced deuteron breakup cases.

#### A. Two-body potentials

In this section we describe the two-body potentials used to represent the  ${}^3\text{He}$ - ${}^3\text{He}$  and  ${}^3\text{He}$ - ${}^3\text{H}$  interaction. We then proceed to describe how Coulomb effects are approximately incorporated in the two-body potentials and three-body calculations. In the Amado (separable potential) model of the Faddeev equations, the matrix elements of the potential are given in momentum space for  $S$ -wave potentials by

$$\langle k | V_i | k' \rangle = -\lambda_i g_i(k) g_i(k') \quad (1)$$

with the  $T$  matrix given by

$$\langle k | T_i(E) | k' \rangle = g_i(k) g_i(k') \tau_i(E), \quad (2)$$

where

$$\tau_i(E) = -\left[ \frac{1}{\lambda_i} + 4\pi \int_0^\infty q^2 \frac{dq g_i^2(q)}{(M/\hbar^2)E - q^2 + i\epsilon} \right]^{-1}.$$

The index  $i$  here just indicates possible spin-isospin quantum numbers. The  $T$  matrix elements of Eq. (2) form the basic input for the Faddeev equations. The relation between the  $T$  matrix and the Faddeev equations for three-body amplitudes appears extensively in the literature to which we refer the reader.<sup>1-5</sup> The  $T$  matrix is related to two-body scattering phase shifts ( $\delta$ ) through its on-shell elements ( $k^2 = k'^2 = ME/\hbar^2$ ) with

$$\langle k | T(k^2 + i\epsilon) | k \rangle = -\frac{1}{2\pi^2 k} e^{i\delta(k)} \sin\delta(k), \quad (3)$$

where  $M$  is the trion mass.

Haftel *et al.*<sup>3,4</sup> have previously used the form factor

$$g_i(k) = N_i \frac{k_{ci}^2 - k^2}{(k^2 + \beta_i^2)^2} \quad (4)$$

in deuteron breakup studies. We adopt the same form in this work. The Yamaguchi form factor [ $g_i(k) \propto 1/(k^2 + \beta_i^2)$ ] used in earlier work is just a special case of this form factor with  $k_{ci}^2 = -\beta_i^2$ .

Whereas the Yamaguchi form factor has proven satisfactory in low energy  $N$ - $N$  scattering, it fails for trion-trion scattering. The reasons are as follows: In the  $N$ - $N$  system the low energy  $S$ -wave scattering results and bound state energy are well represented by two parameters in each spin-isospin state—the scattering length ( $a$ ) and effective range ( $r_0$ ). The success of the effective range formalism in connecting low-energy scattering results with the bound state is intimately connected with the fact that the  $N$ - $N$  interaction supports a barely bound deuteron in the triplet state and a barely unbound virtual state in the singlet state. Not surprisingly potentials with only two parameters (such as  $\lambda$  and  $\beta$  in the Yamaguchi potential) can fit low-energy scattering and the bound state energies. In the trion-trion system the two-body bound states (or resonances) are comparatively deeply bound (15.79 MeV below  ${}^3\text{He} + {}^3\text{H}$  threshold for the  $1^+$  ground state in  ${}^6\text{Li}$ , 12.23 MeV for the first  $0^+$  state in  ${}^6\text{Li}$ , and 11.49 MeV below  ${}^3\text{He} + {}^3\text{He}$  threshold for the  $0^+$  ground state of  ${}^6\text{Be}$ ). In this case an effective range relation is not satisfactory in connecting low-energy scattering with the bound state. Therefore, we would not expect a potential form with only two parameters (like a Yamaguchi) to fit automatically the data and the bound states. Our procedure described below for fitting potentials to the data does not rely on the validity of the effective range formula.

The criterion for choosing a potential was the following: We deemed a potential (such as HS) satisfactory if it (a) gave the correct binding energies of  ${}^6\text{Li}$  and  ${}^6\text{Be}$ , (b) gave an on-shell scattering amplitude which, when the pure Coulomb amplitude was added to it, yielded the  ${}^3\text{He}$ - ${}^3\text{He}$  and  ${}^3\text{He}$ - ${}^3\text{H}$   $90^\circ$  (c.m.) cross sections in approximate agreement with experiment. For the case where both Coulomb and short-range interactions are included, the two-body cross section for nonidentical spinless particles is given by

$$\frac{d\sigma}{d\Omega} = |f_c(\theta) + f_N(\theta)|^2, \quad (5)$$

where

$$f_c(\theta) = \frac{Z_1 Z_2 e^2 M}{4\hbar^2 k^2} \frac{\exp(2i\sigma_0 - i\eta \ln \sin^2 \theta)}{\sin^2 \frac{1}{2} \theta}$$

and for  $S$ -wave potentials

$$f_N(\theta) = e^{-2i\sigma_0} e^{i\delta} \frac{\sin \delta}{k}. \quad (6)$$

In Eqs. (5) and (6)  $\eta = Z_1 Z_2 e^2 M / 2\hbar^2 k$ ,  $\sigma_0 = \arg \Gamma(1 + i\eta)$ , and  $E_{\text{c.m.}} = \hbar^2 k^2 / M$ . In calculating nucleon-nucleon or trion-trion cross sections Eq. (5) is properly modified to take into account spin and statistics.

Our goal was to find a  $g(k)$  such as to produce (approximately)  $f_N(90^\circ)$  as extracted from the trion-trion data [Using Eqs. (5) and (6) modified for proper spin and statistics] with  $g(k)$  related to  $e^{i\delta} \sin \delta / k$  through Eqs. (2) and (3). In other words we have designed a short-range potential that, when inserted alone in the Schrödinger equation gives the experimental (but Coulomb modified) phase shifts. This differs from finding a potential which substituted with the Coulomb forces into the Schrödinger equation gives the experimental (but Coulomb modified) phase shifts. Our separable  $T$  matrix reproduces the correct  $T$  matrix on shell while we have avoided the more complicated problem of incorporating Coulomb interference effects in the construction of the (short range)  $T$  matrix. Two-body Coulomb interference effects, however, are implicitly included (at least on shell) since our procedure fits the experimental data.

Table I gives the potential parameters and properties for one such potential (labeled HS). The information contained in Table I parallels some of the information in Table I of Ref. 4 for  $N$ - $N$  potentials. Since our trion interaction is taken to be charge independent, the charge-dependence labels (e.g.,  $p$ - $p$  and  $n$ - $p$  in Table I of Ref. 4) do not appear and only singlet and triplet sets of parameters are necessary. Like potential HA2-8.3 of Ref. 4, the  $T$  matrix is of the form of Eq. (2), which corresponds to  $\rho(E) = 1$  in the formalism of

TABLE I. Parameters and properties for the potential HS.

Potential parameter	Triplet	Singlet <sup>a</sup>
$k_c^2$ (fm <sup>-2</sup> )	-2.50	-2.50
$\beta$ (fm <sup>-1</sup> )	1.800	2.349
$a$ (fm)	1.698	1.383
$r_0$ (fm)	0.902	0.537
$E_B$ (MeV) <sup>b</sup>	15.793	11.482
$\kappa$ (fm <sup>-1</sup> ) <sup>c</sup>	1.0675	0.9102
$\lambda N^2$ (fm <sup>-3</sup> )	2.2797	5.4675

<sup>a</sup>The singlet interaction is taken to be charge-independent due to the closeness of the binding energies of the lowest  $0^+$  states in  ${}^6\text{Li}$  and  ${}^6\text{Be}$ .

<sup>b</sup>For the triplet state this is the binding energy of  ${}^6\text{Li}$  and for the singlet state this is the binding energy of  ${}^6\text{Be}$ .

<sup>c</sup>This is the  $\kappa$  parameter of Ebenhöh which the code uses in favor of  $\lambda$ .

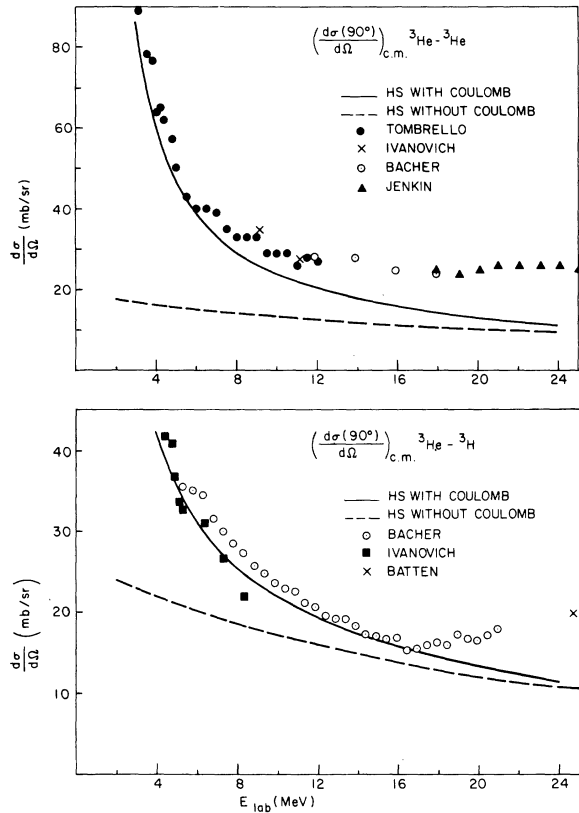


FIG. 1. Comparison of the experimental  $90^\circ$  c.m. two-body scattering cross sections, for (a)  ${}^3\text{He}-{}^3\text{He}$  and (b)  ${}^3\text{He}-{}^3\text{H}$  with the cross section predictions of the HS model. The dashed curve is the HS model prediction, while the solid curve has the Coulomb amplitude included. Experimental data are those listed in Table II.

Ref. 4. While other potentials could be designed that give virtually identical fits to the two-body data for  $E_{\text{lab}} > 3$  MeV (but with different  $a$  and  $r_0$ ) we only consider potential HS in this investigation.

Figures 1(a) and 1(b) illustrate the  ${}^3\text{He}-{}^3\text{He}$  and  ${}^3\text{He}-{}^3\text{H}$  two-body  $90^\circ$  (c.m.) cross sections of the separable model HS compared with experiment. The solid curves represent fits when the Coulomb amplitude is included while the dashed curves give the cross sections predicted by just the pure S-wave separable potential. Without the Coulomb interaction the HS potential gives the  ${}^3\text{He}-{}^3\text{He}$   $90^\circ$  (c.m.) cross sections of about 40% of the experimental values in the region 6–20 MeV (lab). In  ${}^3\text{He}-{}^3\text{H}$  the cross sections are about 70–80% of the experimental values. Figures 2(a) and 2(b) show the  ${}^3\text{He}-{}^3\text{He}$  and  ${}^3\text{He}-{}^3\text{H}$  angular distributions at various energies. The fits are generally poor because of the neglect of higher partial waves and (for HS without Coulomb) the Coulomb interaction. Interestingly, we shall see later that the  ${}^3\text{He}-{}^3\text{He}$  and  ${}^3\text{He}-{}^3\text{H}$  QFS cross sections predicted by the

Ebenhöh code have roughly the same ratios with respect to experimental cross sections as the cross sections in Fig. 1 (dashed curves) have to the experimental two-body cross sections.

With the Coulomb amplitude added to that of HS, good fits are obtained in the  ${}^3\text{He}-{}^3\text{He}$  system up to about 12 MeV (lab) while in  ${}^3\text{He}-{}^3\text{H}$  good fits occur up to 20 MeV (lab) for  $90^\circ$  (c.m.) cross sections. Therefore we conclude that the potential HS provides a fairly accurate representation of the hadronic S-wave trion-trion  $T$  matrix (at least on-shell). At this point we might speculate that if the Coulomb interactions were included in the breakup code the predicted cross sections for the QFS region would improve because of the importance of the Coulomb force in the two-body interaction. As discussed later, we actually find that the approximate inclusion of the Coulomb interaction does improve the magnitudes of QFS cross sections, but the improvement is not nearly as drastic as in the two-trion scattering. Surprisingly, the pure HS potential gives a remarkably good fit to the shapes of the QFS spectrum; better than one might expect

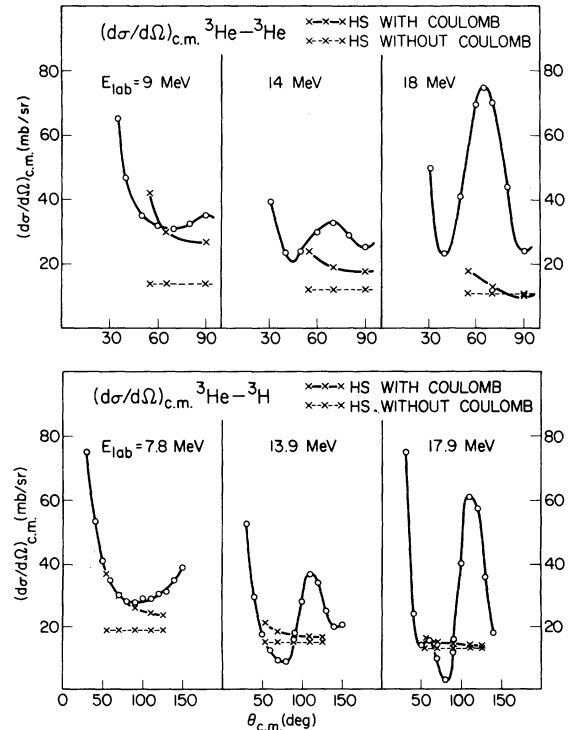


FIG. 2. Comparison of the experimental angular distributions for (a) the  ${}^3\text{He}-{}^3\text{He}$  and (b)  ${}^3\text{He}-{}^3\text{H}$  reactions with the calculations using the HS model. The dashed curve is the HS model prediction, while the solid curve has the Coulomb amplitude included. Experimental data are those listed in Table II and are connected here by a solid line to aid the eye.

on the basis of the fits of the HS potential to the trion-trion elastic scattering data. In particular, the experimental trion-trion elastic scattering angular distributions are not adequately described [ Figs. 2(a) and 2(b)] by the HS model either with or without Coulomb interaction. The approximate inclusion of the Coulomb interaction, however, makes the QFS shapes somewhat worse.

Once the two-body  $T$  matrix is found for potential HS, we employ this as the basic input for the Haftel modified version of the Ebenhöf code. From the code breakup amplitudes are calculated assuming the full trion-trion potential to be the HS potential. We then calculate cross sections both with and without the Coulomb corrections.

### B. Calculation of Coulomb effects in breakup

The Coulomb force plays a far greater role in trion-trion scattering than in  $N$ - $N$  scattering. Presumably it will also be much more important in the present  ${}^6\text{Li}$  breakup reaction than in  $p$ - $d$  breakup. Furthermore, since we have employed the Coulomb amplitude in calculating cross sections for our potential fits, consistency would require a similar procedure in the three-body calculation.

We consider three types of corrections to approximate the effect of the Coulomb force. The first two modify the phase and low energy behavior of the Faddeev amplitudes calculated from the code. These types of corrections have previously been treated by Bruinsma *et al.*<sup>24</sup> A third correction, not previously considered in breakup reactions, is to add the single scattering Coulomb amplitudes (Born terms) to the Faddeev amplitudes. These amplitudes, which are taken suitably off shell, reflect the anisotropy of the two-body cross sections which is not reflected in the corrections considered previously.<sup>24</sup>

Consider the Faddeev amplitude  $T_\sigma^S(i)$  [we use the notation of Eqs. (12) and (13) of Ref. 4] which represents particles  $j$  and  $k$  ( $i \neq j \neq k$ ) interacting last. The first term of the multiple scattering series (Born term) is composed of the half shell two-body  $T$  matrix element and the bound state wave function  $\psi_B(\vec{p}_{0i})$ , i.e.,

$$[T_\sigma^S(i)]_{\text{Born}} \propto T_{i\sigma}(\vec{p}_i, \vec{p}'_i; p_i^2 + i\epsilon)\psi_B(\vec{p}_{0i}), \quad (7)$$

where  $\vec{p}_i$  is the final relative momentum of particles  $j$  and  $k$  and where  $i \neq j > k \neq i$  and

$$\vec{p}_i = \epsilon_{ijk}(\vec{k}_j - \vec{k}_k)/2,$$

$$\vec{p}'_i = -\epsilon_{ijk} \frac{2}{\sqrt{3}} (\vec{q}_0 + \frac{1}{2} \vec{q}_i),$$

$$\vec{p}_{0i} = \epsilon_{ijk} \frac{2}{\sqrt{3}} (\frac{1}{2} \vec{q}_0 + \vec{q}_i),$$

$$q_0^2 = \left( \frac{M}{\hbar^2} E + \kappa_0^2 \right), \quad q_i^2 = \left( \frac{M}{\hbar^2} E - p_i^2 \right),$$

$$\epsilon_{ijk} = \begin{cases} +1 & \text{if } ijk \text{ are cyclic,} \\ -1 & \text{if } ijk \text{ are not cyclic.} \end{cases}$$

Here  $-\hbar^2 \kappa_0^2 / M$  is the bound state energy,  $\vec{q}_0$  is directed opposite the initial projectile momentum (in the c.m. frame), and  $\vec{q}_i$  is directed opposite to  $\vec{k}_i$  (momentum of particle  $i$ ). For on-shell scattering ( $p_i^2 = p_i'^2$ ) the Coulomb force modifies the phase of the two-body amplitude by a phase factor  $e^{2i\sigma_i(p_i)}$  where  $\sigma_i(p) = \arg \Gamma[1 + i\eta_i(p)]$ ,  $\eta_i(p) = Z_j Z_k e^2 M / 2\hbar^2 p$ . Bruinsma *et al.*<sup>24</sup> have noted that for half-off-shell scattering appropriate to Eq. (7) the phase factor becomes  $\exp\{i[\sigma_i(p_i) + \sigma_i(p'_i)]\}$ , i.e.,

$$T_\sigma^S(i) \rightarrow \exp\{i[\sigma_i(p_i) + \sigma_i(p'_i)]\} T_\sigma^S(i).$$

We incorporate this phase change in our calculations.

The second Coulomb effect shows up in the low-energy behavior of the two-body force. For normal short-range interactions the two-body on-shell amplitude is proportional to  $e^{i\delta} \sin\delta/k$ , where  $\delta$  is the phase shift and the phase shifts obey the effective range formula at low energy:

$$k \cot\delta \simeq -\frac{1}{a} + \frac{1}{2} r_0 k^2. \quad (8)$$

Since the two-body forces inserted in the code are  $S$ -wave short-range interactions, their predicted phase shifts obey such a relation (at least at very low energies). However, because of Coulomb interference effects, the actual (Coulomb modified) phase shifts  $\delta'$  do not obey such a simple quadratic relation but rather

$$k \cot\delta' \simeq \frac{e^{2\pi\eta(k)} - 1}{2\pi\eta(k)} \left[ -\frac{1}{a_c} + \frac{1}{2} r_{0c} k^2 - 2k\eta(k)h(\eta) \right], \quad (9)$$

where  $h(\eta) = \eta^2 \sum_{n=1}^{\infty} 1/[n(n^2 + \eta^2)] - \ln\eta - 0.57722\dots$  and  $a_c$  and  $r_{0c}$  are experimental effective range parameters. Note, for example, that  $e^{i\delta} \sin\delta / k \xrightarrow{k \rightarrow 0} 0$  for the Coulomb case while it goes to  $-a$  for a short-range interaction. To incorporate this low-energy behavior into the calculation (especially in the  $p$ - $p$  FSI region) Bruinsma *et al.*<sup>24</sup> multiply  $T_\sigma^S(i)$  by a factor

$$F_c(p_i) = e^{i\delta'} \sin\delta' / e^{i\delta} \sin\delta, \quad (10)$$

$$T_\sigma^S(i) \rightarrow F_c(p_i) T_\sigma^S(i).$$

Here  $\delta'$  is the phase shift calculated according to Eq. (9) while  $\delta$  is the phase shift calculated according to Eq. (8). The potentials in Ref. 24 are fitted to the experimental effective range param-

eters and therefore they use  $a = a_c$  and  $r_0 = r_{0c}$ . Of course, one can question the wisdom of applying this factor  $F_c(p_i)$  to the final amplitude rather than in the input  $T$  matrix elements. The final results, however, well reproduce the minima at the  $p$ - $p$  FSI.

With our potentials we directly fit amplitudes to the data in a region beyond which the effective range formula is valid ( $E_{\text{lab}} \geq 3$  MeV). In the region considered our  $T$  matrices have the right energy dependence, at least on shell. Nevertheless, the very low-energy limit is incorrect, since the experimental very low energy phase shifts would obey a Coulomb modified effective range relation and HS is, after all, a short range potential. Following Bruinsma *et al.*<sup>24</sup> we introduce in the code a factor  $F_c(p_i)$  as given in Eq. (10) with

$$\frac{\cot \delta'}{\cot \delta} = \begin{cases} 1 + [1 - \rho_c(p_i)] [(E - E_0)/E_0] & \text{for } E \leq E_c, \\ 1 & \text{for } E > E_c, \end{cases} \quad (11a)$$

where  $E = \hbar^2 p_i^2 / M$ ,  $E_c = 1.5$  MeV (the c.m. energy at which we began our fit) and

$$\rho_c(p) = \frac{e^{2\pi\eta(p)} - 1}{2\pi\eta(p)} \left[ -\frac{1}{a'} + \frac{1}{2} r'_0 p^2 - 2p\eta(p)h(p) \right] \times \left[ -\frac{1}{a} + \frac{1}{2} r_0 p^2 \right]^{-1}. \quad (11b)$$

In Eq. (11b)  $r_0$  and  $a$  are the effective range parameters of the potential used, and ideally  $r'_0$  and  $a'$  are the experimental values. Trion-trion effective range parameters are actually unknown but we tried to extract them from the data as best we could. Actually, for most of the region of phase space examined,  $\hbar^2 p_i^2 / M > E_c$  and for all practical purposes  $F_c(p_i)$  was always unity. Note that in order to conform with the notation used in previous references we use  $p$  and  $q$  as wave numbers (i.e., as " $k$ ").

Finally we added the single scattering Coulomb terms into the breakup amplitudes. Following Bajzer's derivation<sup>25</sup> of the on-shell Coulomb amplitude, but extending it to half-off-energy shell scattering, we arrive at the result<sup>26</sup>

$$f_{ci}(p_i, p'_i) = \frac{\Gamma(1+i\eta)}{\Gamma(1-i\eta')} \left[ e^{\pi/2(\eta-\eta')} \frac{(4p_i'^2)^{i\eta'}}{q^{2i\eta}} \frac{Z_j Z_k e^2 M}{q^2 \hbar^2} \times (p_i^2 - p_i'^2)^{i(\eta-\eta')} \right], \quad (12)$$

where  $\eta$  and  $\eta'$  are shorthand for  $\eta_i(p_i)$  and  $\eta_i(p'_i)$  and  $q^2 = (\vec{p}_i - \vec{p}'_i)^2$ . In a form more amenable to the code our Coulomb correction amounts to adding a term  $T_{\sigma c}^S(i)$  to  $T_{\sigma}^S(i)$  of Eq. (10), with

$$T_{\sigma c}^S(i) = -4\Lambda_{\sigma 0}^S e^{i(\sigma_i + \sigma'_i)} (1 - \delta_{1i}/2) R_i(p_i, p'_i) \times [e^{-i\eta \ln q_i^2} + V_{ci}(q_i^2) + (-1)^{\sigma+1} \delta_{1i} e^{-i\eta \ln q_i^2} - V_{ci}(q_i^2)] \psi_B(\vec{p}_0), \quad (13)$$

where  $\sigma_i$  and  $\sigma'_i$  correspond to  $\sigma_i(p_i)$  and  $\sigma_i(p'_i)$ , respectively. The  $\Lambda_{\sigma 0}^S$  are the spin recoupling coefficients (see Table II of Ref. 5) and

$$R_i(p, p') = \left[ \frac{\eta}{\eta'} \frac{1 - e^{-2\pi\eta'}}{1 - e^{-2\pi\eta}} \right]^{1/2} \times \exp[i\eta' \ln(4p_i'^2) + (\eta - \eta') \times (-\pi + i \ln(p_i'^2 - p_i^2))], \quad p_i'^2 > p_i^2,$$

$$V_{ci}(q^2) = \frac{Z_j Z_k e^2 M}{2\pi^2 q^2 \hbar^2} \quad \text{and} \quad q_i \pm = (\vec{p}_i \mp \vec{p}'_i)^2.$$

The factors involving  $\delta_{1i}$  and  $(-1)^{\sigma+1}$  ( $\sigma=0$  spin triplet,  $\sigma=1$  spin singlet) reflect the Pauli principle where the two like particles (in our case two  ${}^3\text{He}$ ) are pair 1 (i.e., particles 2 and 3). The expression for the cross section is similar to Eq. (12) of Ref. 4 except now there is an additional amplitude  $T_{\sigma=0, pp}^S$  the triplet  $p$ - $p$  (i.e.,  ${}^3\text{He}$ - ${}^3\text{He}$ ) interaction which in our model only has a Coulomb part. The modification to Eq. (12) of Ref. 4 becomes

$$\frac{d^3\sigma}{d\Omega_1 d\Omega_2 dE_1} = (|M_{D1}|^2 + |M_{D2}|^2 + |M_Q|^2) \times (\text{kinematic factors}),$$

$$M_{D1} = \frac{1}{3} T_{0pp}^{1/2}(1) + \frac{\sqrt{3}}{12} [T_{1np}^{1/2}(2) - T_{1np}^{1/2}(3) + T_{0np}^{1/2}(2) - T_{0np}^{1/2}(3)],$$

$$M_{D2} = \frac{1}{3} [T_{1pp}^{1/2}(1) + \frac{1}{4} T_{1np}^{1/2}(2) + \frac{1}{4} T_{1np}^{1/2}(3) - \frac{3}{4} T_{0np}^{1/2}(2) - \frac{3}{4} T_{0np}^{1/2}(3)],$$

$$M_Q = -\frac{\sqrt{2}}{3} T_{0pp}^{1/2}(1) + \frac{1}{\sqrt{6}} [T_{0np}^{3/2}(2) - T_{0np}^{3/2}(3)].$$

Of course, here  $p$  stands for  ${}^3\text{He}$  and  $n$  for  ${}^3\text{H}$ . This equation differs from Eq. (12) of Ref. 4 in that the  $p$ - $p$  pair is  $i=1$  (in Ref. 4 it is  $i=3$ ) and the presence of the Coulomb  $\sigma=0$  spin triplet  $p$ - $p$  terms.<sup>26</sup>

In summary we have included the Coulomb force in a quasi-two-body fashion. We include modifications of the phase and low-energy behavior of the strong interaction Faddeev amplitudes as we would modify half-off-energy shell two-body amplitudes. We have also added the half-off-energy shell Coulomb amplitude relevant for the single scattering term in the multiple scattering series. To include it in all multiple scatterings would require a meth-

od to integrate the Coulomb interaction in the Faddeev equations such as the method of Alt *et al.*<sup>27,28</sup> Alt *et al.*<sup>28</sup> have recently applied this method to *p-d* elastic scattering but not as yet to breakup. To apply it to breakup is a more complicated procedure and could not be easily included in the currently available breakup codes.

### C. Plane-wave impulse approximation

The plane-wave impulse approximation (PWIA) used in this work is described in detail in Ref. 23. The cross section for the reactions  ${}^6\text{Li}({}^3\text{He}, {}^3\text{He}, {}^3\text{He}){}^3\text{H}$  or  ${}^6\text{Li}({}^3\text{He}, t){}^3\text{He}$  is given by

$$\frac{d^3\sigma}{d\Omega_3 d\Omega_4 dE_3} = \sigma_{\text{free}} |\text{FT}|^2 \text{KF}.$$

The quantity  $\sigma_{\text{free}}$  is the trion-trion free elastic scattering cross section calculated on shell in the post collision energy approximation. The square of the Fourier transform of the  ${}^6\text{Li}$  wave function

is  $|\text{FT}|^2$ . The nucleus  ${}^6\text{Li}$  is described as composed of two clusters  ${}^3\text{He}$  and  ${}^3\text{H}$ . The wave function used is given by

$$N \frac{e^{-\epsilon r} - e^{-\beta r}}{r},$$

where  $\beta = 1.202 \text{ fm}^{-1}$  and the quantity  $g$  is related to the  ${}^3\text{He}$ - ${}^3\text{H}$  binding energy in  ${}^6\text{Li}$ . The kinematic factor is KF. The  ${}^3\text{He}$ - ${}^3\text{He}$  and  ${}^3\text{He}$ - ${}^3\text{H}$  elastic scattering data used in the PWIA analysis are summarized in Table II.

## IV. RESULTS

The predictions of our three models: (1) three-body separable potential (HS), (2) three-body separable potential modified by the Coulomb interaction as described in Sec. III (HS+C), and (3) PWIA are shown in Figs. 3(a) and 3(b) for the kinematic conditions of the trion-trion QFS ( $28.3^\circ$ - $28.3^\circ$ ). Due to the large trion-trion binding energy

TABLE II. Summary of the  ${}^3\text{He}$ - ${}^3\text{He}$  and  ${}^3\text{He}$ - ${}^3\text{H}$  elastic scattering data used in the PWIA analyses.

Reaction	Energy (c.m.) (MeV)	Angle (c.m.) (deg)	References
${}^3\text{He}({}^3\text{He}, {}^3\text{He}){}^3\text{He}$	2.95	$40^\circ$ - $90^\circ$	Tombrello and Bacher <sup>a</sup>
	3.95	$35^\circ$ - $90^\circ$	
	4.96	$30^\circ$ - $90^\circ$	
	5.96	$31^\circ$ - $90^\circ$	Ivanovich and Young <sup>b</sup>
	4.54	$30^\circ$ - $90^\circ$	
	5.54	$30^\circ$ - $90^\circ$	
	6.94	$30^\circ$ - $90^\circ$	
	7.95	$30^\circ$ - $90^\circ$	Bacher <i>et al.</i> <sup>c</sup>
	8.95	$30^\circ$ - $90^\circ$	
	10.0	$25^\circ$ - $90^\circ$	Jenkin <i>et al.</i> <sup>d</sup>
${}^3\text{H}({}^3\text{He}, {}^3\text{He}){}^3\text{H}$	2.24	$40^\circ$ - $140^\circ$	Ivanovich <i>et al.</i> <sup>e</sup>
	2.5	$40^\circ$ - $140^\circ$	
	3.1	$40^\circ$ - $140^\circ$	
	3.2	$50^\circ$ - $150^\circ$	
	3.5	$40^\circ$ - $140^\circ$	
	4.0	$40^\circ$ - $140^\circ$	
	4.5	$40^\circ$ - $140^\circ$	
	5.0	$40^\circ$ - $140^\circ$	
	5.2	$30^\circ$ - $150^\circ$	Bacher <i>et al.</i> <sup>f</sup>
	7.2	$30^\circ$ - $150^\circ$	
	9.2	$54^\circ$ - $125^\circ$	
	10.0	$30^\circ$ - $126^\circ$	
	10.7	$30^\circ$ - $126^\circ$	
	13.8	$31^\circ$ - $175^\circ$	Batten <i>et al.</i> <sup>g</sup>
16.2	$50^\circ$ - $170^\circ$		

<sup>a</sup> T. A. Tombrello and A. D. Bacher, *Phys. Rev.* **130**, 1108 (1963).

<sup>b</sup> M. Ivanovich, P. G. Young, and G. G. Ohlsen, *Nucl. Phys. A* **110**, 441 (1968).

<sup>c</sup> A. D. Bacher, R. J. Spiger, and T. A. Tombrello, *Nucl. Phys. A* **119**, 481 (1968).

<sup>d</sup> J. A. Jenkin, W. D. Harrison, and R. E. Brown, *Phys. Rev. C* **1**, 1622 (1970).

<sup>e</sup> M. Ivanovich, P. G. Young, and G. G. Ohlsen, *Nucl. Phys. A* **110**, 441 (1968).

<sup>f</sup> A. D. Bacher, R. J. Spiger, and T. A. Tombrello, *Nucl. Phys. A* **119**, 481 (1968).

<sup>g</sup> R. J. Batten, D. L. Clough, J. B. A. England, R. G. Harris, and D. H. Worledge, *Nucl. Phys. A* **151**, 56 (1970).



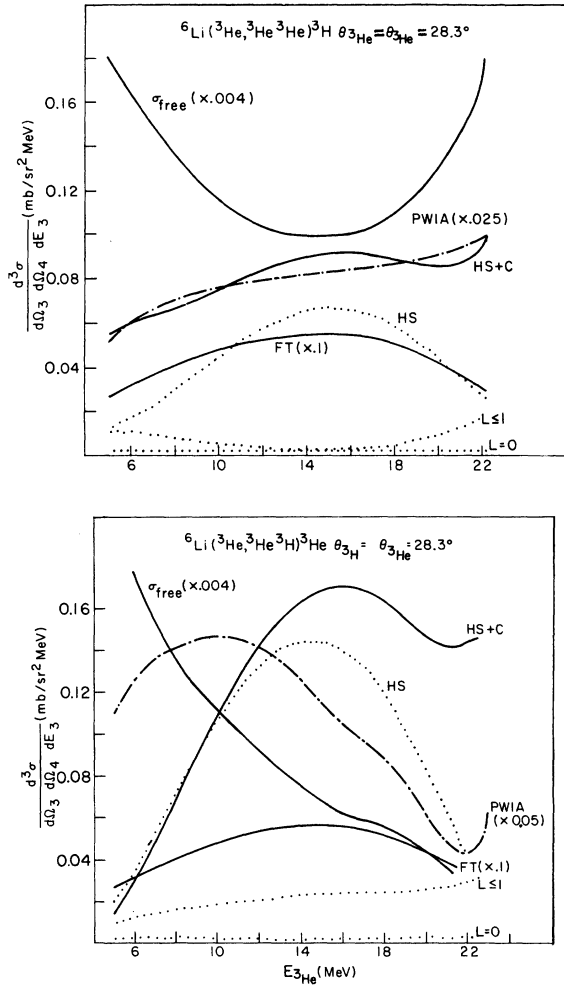


FIG. 3. This figure shows the three model predictions. The curve labeled HS+C and HS represent the separable potential three-body predictions with and without the Coulomb interaction, respectively. The PWIA prediction is also shown along with the Fourier transform (FT) and free cross section  $\sigma_{free}$  associated with it. In addition the bottom two dotted curves show the HS model cross sections when only  $L=0$  and  $L=1$  are included ( $L$  is the  ${}^6\text{Li}$ -trion relative orbital angular momentum).

the square of the Fourier transform of the  ${}^6\text{Li}$  cluster wave function ( ${}^3\text{H} + {}^3\text{He}$ ) is essentially flat as a function of  $E_3$ , the energy of the detected  ${}^3\text{He}$ , though the momentum transfer changes from  $0.04 \text{ fm}^{-1}$  at 14 MeV to  $0.45 \text{ fm}^{-1}$  at 22 and 6 MeV. Consequently, the  $E_3$  dependence of the PWIA cross section is mainly determined by the free trion-trion cross section. We have used the free cross section in the post collision energy prescription. The two-body c.m. energy decreases from about 8 MeV to 6.5 MeV at the minimum momentum transfer and then increases again while the c.m.

angle decreases from  $115^\circ$  to  $65^\circ$  ( $90^\circ$  being at the minimum momentum transfer). The  ${}^3\text{He} + {}^3\text{He}$  free cross section has to be symmetric with respect to  $90^\circ$ , while the  ${}^3\text{He} + {}^3\text{H}$  cross section is not symmetric around  $90^\circ$ . The strong variation of the free  ${}^3\text{He} + {}^3\text{H}$  cross section as  $E_3$  increases causes the PWIA cross section peak to shift by about 5 MeV. The prediction of the cross section using the HS potential peaks close to the minimum momentum transfer and the shape of the curve is narrower than the shape of the square of the Fourier transform. This shape is partly due to the decrease of the c.m. energy of the two trions undergoing QFS, which results in the increase in the trion-trion cross section and partly to the strong interferences describing the absorption inside the  ${}^6\text{Li}$  nucleus. Indeed, using a cutoff radius of 3 fm the square of the Fourier transform produces a shape comparable to the HS results. However, for the  $20^\circ$ - $20^\circ$  angle pair the transferred momentum changes very little in the region of interest and thus the shape of the Fourier transform is not materially changed by a cutoff radius even though the magnitude is decreased. The need for some absorption is shown in the data for the  $35^\circ$ - $35^\circ$  angle pair where the two-body c.m. energy is constant throughout the spectrum.

Figures 3(a) and 3(b) also show the cross sections for the HS potential retaining only  $L=0$  and  $L=1$  Faddeev amplitudes ( $L$  is the  ${}^6\text{Li}$ -trion,  ${}^6\text{Be}$ -trion, or  ${}^6\text{Li}^*$ -trion relative orbital angular momentum). Similarly to the nucleon induced deuteron breakup one can see that the  $L=0$  contributions to the QFS cross sections are small (1-2%).<sup>4</sup> Note, however, a significant increase occurs in the cross section for ( ${}^3\text{He}, t^3\text{He}$ ) when  $L=1$  is included which does not occur for ( ${}^3\text{He}, {}^3\text{He}^3\text{He}$ ).

The cross sections predicted by the separable HS potential model modified by the Coulomb interaction are also shown in Figs. 3(a) and 3(b). The inclusion of the Coulomb modification increases the ( ${}^3\text{He}, {}^3\text{He}^3\text{He}$ ) cross section by about 25-100%. The effect becomes larger for conditions away from QF scattering, which can be understood by noting that  $\theta_{3\text{He}^3\text{He}}$  is  $90^\circ$  at the QFS and decreases away from QFS and, of course, in our Coulomb modified model the  ${}^3\text{He} + {}^3\text{He}$  cross section increases when  $\theta_{3\text{He}^3\text{He}}$  decreases. For the reaction ( ${}^3\text{He}, t^3\text{He}$ ) the inclusion of the Coulomb modification produces a much smaller effect up to  $E_3 = 15 \text{ MeV}$  ( $\theta_{t^3\text{He}} = 90^\circ$ ) and only for larger  $E_3$  (corresponding to  $\theta_{t^3\text{He}} = 90^\circ$ - $60^\circ$ ) does the effect become larger. It is worthwhile to point out that while the Coulomb interaction significantly changes the trion-trion cross section (see Figs. 1 and 2), its effect on the breakup is much smaller. It looks as if the influence of the longer-range part of the

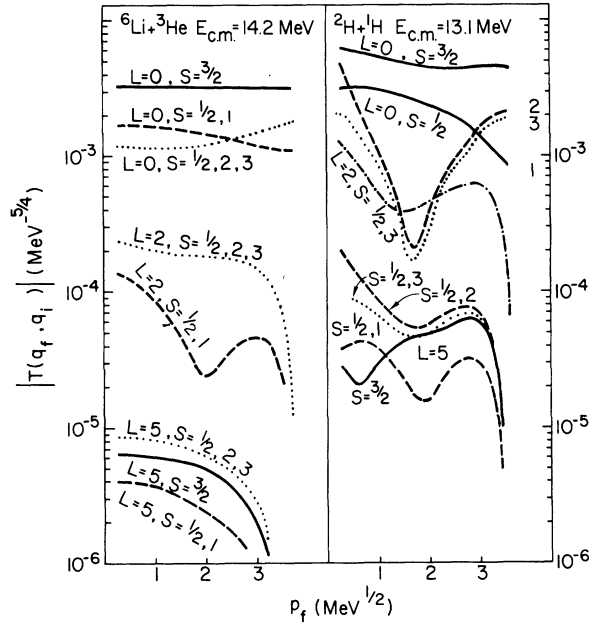


FIG. 4. Breakup amplitudes in various spin and angular momentum states. The labels 1, 2, and 3 indicate, respectively, the spectator particle plus two-body subsystems:  ${}^3\text{He} + (t^3\text{He})_{\text{triplet}}$ ,  ${}^3\text{He} + (t^3\text{He})_{\text{singlet}}$ , and  ${}^3\text{H} + ({}^3\text{He}^3\text{He})_{\text{singlet}}$ , and in an analogous way for the  $p+d$  system. For the  ${}^3\text{He} + {}^6\text{Li}$  system the assumed charge independence makes 2 and 3 identical. Here  $p_f$  is the relative momentum in the two-body subsystem.

interaction is suppressed in the three-body breakup process.

Figure 4 shows the breakup amplitude in various spin and angular momentum states and compares the results for the reaction  ${}^6\text{Li} + {}^3\text{He}$  at  $E_{\text{c.m.}} = 14.21$  MeV (corresponding to  $E_{\text{inc}} = 45$  MeV) to those for the reaction  $d+p$  at  $E_{\text{c.m.}} = 13.11$  MeV (corresponding to  $E_{\text{inc}} = 23$  MeV). In this figure  $p_f$  is the relative momentum of the two-body subsystem (referred as  $d$ ,  $d^*$  or  ${}^6\text{Li}$ ,  ${}^6\text{Li}^*$ , respectively), here  $E_{\text{c.m.}} = \frac{2}{3}E_{1\text{ab}} - Q$ .  $S$  is the total spin. The  ${}^6\text{Li}$ -trion amplitudes are considerably less  $p_f$  dependent than  $d$ - $p$  amplitudes. The higher orbital angular momentum amplitudes are smaller for the  ${}^6\text{Li}$ -trion than for the  $d$ - $p$  system, reflecting the larger binding energy of the two trions in  ${}^6\text{Li}$  than of two nucleons in  $d$ . The relative contribution of the  $L=0$ ,  $S=\frac{1}{2}$  amplitudes is larger for the  ${}^6\text{Li}$ -trion system than for the  $d$ - $p$  system. Since these amplitudes are more sensitive to changes in the short-range particle-particle interaction,<sup>4</sup> one can expect that the  ${}^6\text{Li} + {}^3\text{He} \rightarrow {}^3\text{He} + {}^3\text{He} + {}^3\text{H}$  cross sections in certain regions of the phase space are quite sensitive to the short range trion-trion interaction.<sup>12</sup>

The experimental data will now be compared with the theory. In all of the experimental results the data points have been projected from the kinematic

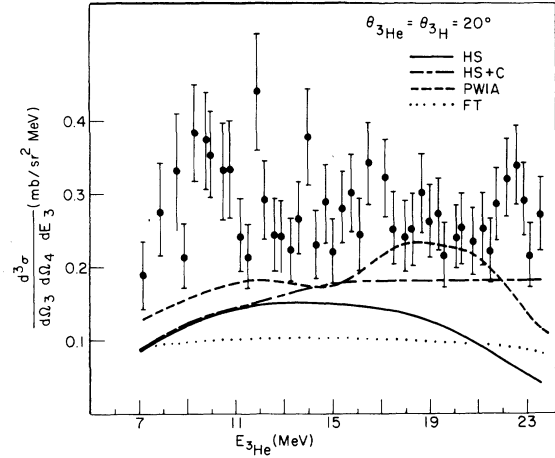


FIG. 5. Comparison of the  ${}^6\text{Li}({}^3\text{He}, t^3\text{He}){}^3\text{He}$  experimental data with theoretical calculations for  $\theta_{3\text{He}} = \theta_{3\text{H}} = 20^\circ$ . The curves labeled HS + C (dashed-dotted) and HS (solid) are the HS model three-body cross section calculations with and without Coulomb interaction, respectively. The curve labeled FT (dotted) represents the square of the Fourier transform associated with the PWIA model. The PWIA calculation (dashed) is normalized by  $N = 0.06$ .

locus onto the  ${}^3\text{He}$  axis. Figures 5–7 represent the results of the  ${}^6\text{Li}({}^3\text{He}, t^3\text{He}){}^3\text{He}$  reaction at  $\theta_{3\text{He}} = \theta_{3\text{H}} = 20^\circ$ ,  $28.3^\circ$ , and  $35^\circ$ , respectively, while Figs. 8–10 show the results for  ${}^6\text{Li}({}^3\text{He}, {}^3\text{He}^3\text{He}){}^3\text{H}$  at  $\theta_{3\text{He}} = \theta_{3\text{H}} = 20^\circ$ ,  $28.3^\circ$ , and  $35^\circ$ , respectively.

The solid, dot-dashed, and dashed curves are the results of the HS, HS + C, and PWIA models. The superiority of the Faddeev type models is immediately obvious. Both HS and HS + C models reproduce reasonably well the absolute cross section, while the PWIA requires normalization constants of  $N \approx 0.06$  and  $N \approx 0.03$  for the reactions

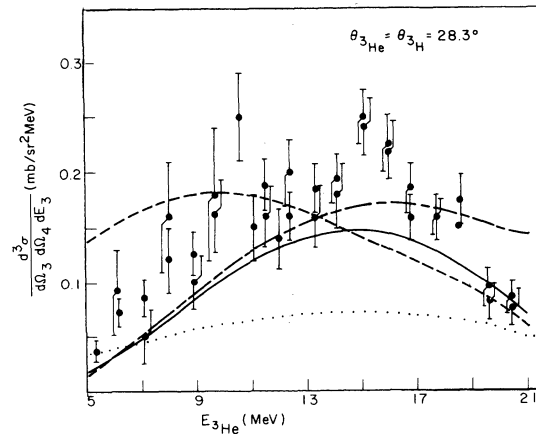


FIG. 6. Same as Fig. 5 for  $\theta_{3\text{He}} = \theta_{3\text{H}} = 28.3^\circ$ . This is the quasifree scattering pair.

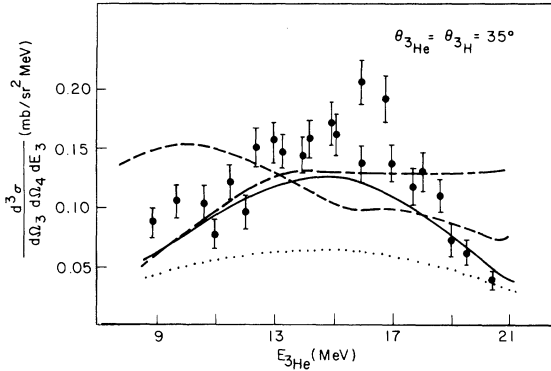


FIG. 7. Same as Fig. 5 for  $\theta_{3\text{He}} = \theta_{3\text{H}} = 35^\circ$ .

( $^3\text{He}, t^3\text{He}$ ) and ( $^3\text{He}, ^3\text{He}^3\text{He}$ ), respectively. Actually, at the QFS condition the HS model underestimates the experimental cross section by 30%, and the HS+C model by about 10–20% for both reactions. The ratio of the normalization factors required in the PWIA for ( $^3\text{He}, t^3\text{He}$ ) and ( $^3\text{He}, ^3\text{He}^3\text{He}$ ) reactions is two and this is the same trend observed in the  $d(p, pn)p$  vs  $d(p, pp)n$  cross sections. It again demonstrates the same inadequacy of the PWIA, and the explanation is in terms of Faddeev type models which properly take the spin and isospin into account. One can state that these simple three-body models predict the ratio of the cross sections better than the individual absolute values.

Not only the absolute magnitudes but even the shapes of the spectra are better predicted by the Amado model calculations. In particular for the ( $^3\text{He}, t^3\text{He}$ ) reaction the PWIA does not give good agreement with the data. This is because the PWIA cross section is here dominated by the free trion-trion cross sections. However, the fluctuations of this free cross section are not reflected in the ex-

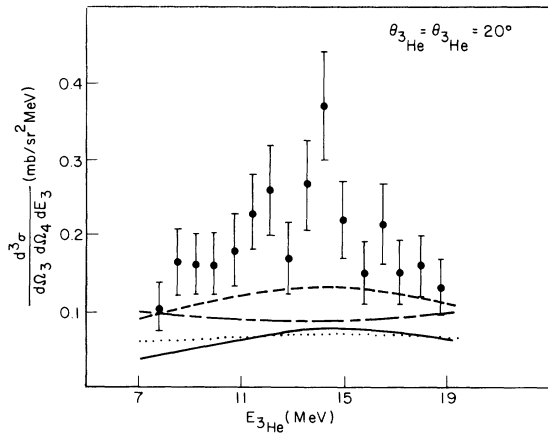


FIG. 8. Same as Fig. 5 but for the reaction  $^6\text{Li}(^3\text{He}, ^3\text{He}^3\text{He})^3\text{H}$  and  $N=0.03$  at  $\theta_{3\text{He}} = \theta_{3\text{He}} = 20^\circ$ .

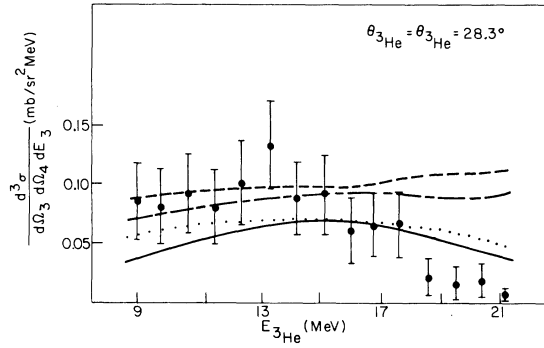


FIG. 9. Same as Fig. 8 for  $\theta_{3\text{He}} = \theta_{3\text{He}} = 28.3^\circ$ . This is the quasifree scattering angle pair.

perimental breakup data. The generally smooth behavior of the spectra may be associated with the strong binding of the trions in the  $^6\text{Li}$  and therefore the peripheral nature of the process is no longer dominant. Also, since the  $^6\text{Li}$  binding energy is 15 MeV, the interaction is considerably off shell which could change the PWIA results. Since the half-off-shell cross sections have not yet been calculated we do not consider them. Our present theoretical results differ from those in Ref. 12 in two respects: (i) the use of the Haftel form factor<sup>3,4</sup> instead of the Yamaguchi form factor and (ii) the singlet interaction is assumed to be charge independent and related to the bound state of the two trions (Ref. 12 uses the negative scattering length). An error in the second part of the Ebenh oh code as applied to this reaction has been found and corrected.

Our Coulomb modification of the HS model provides only an estimate of the total effect of the Coulomb force. For better results, the Coulomb interaction should be correctly included in the Faddeev treatment. Therefore, one should not attach too much meaning to the comparison of the HS+C model with the data. The ratio of the experimental vs HS and HS+C cross sections are

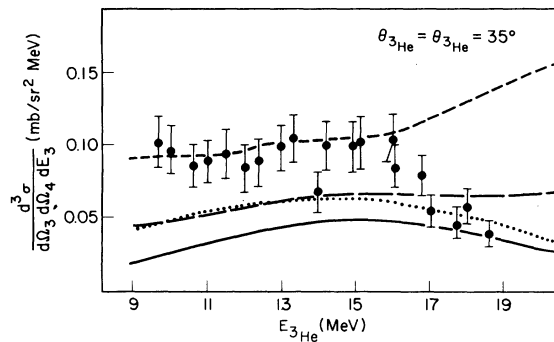


FIG. 10. Same as Fig. 8 for  $\theta_{3\text{He}} = \theta_{3\text{He}} = 35^\circ$ .

TABLE III. Ratio of the experimental vs the calculated cross sections at the minimum momentum transfer.

$\theta_3 = \theta_4$	$({}^3\text{He}, t{}^3\text{He})$	$({}^3\text{He}, t{}^3\text{He})$	$({}^3\text{He}, {}^3\text{He}{}^3\text{He})$	$({}^3\text{He}, {}^3\text{He}{}^3\text{He})$
	HS	HS + C	HS	HS + C
20°	1.7	1.4	3.7	3.3
28.3°	1.3	1.2	1.3	1.1
35°	1.3	1.2	2.0	1.5

shown in Table III. The experimental cross sections are larger than the calculated cross sections typically by 10–50%. The notable exceptions occur at the 20°–20° data where the experimental cross sections are 1.7 to 4 times larger than the Amado model prediction. It should be noted that the 20°–20° data also require larger normalization constants in the PWIA model. It seems that the HS + C model provides a somewhat better agreement with the absolute experimental cross section and a somewhat worse fit to the shape of the spectra than the HS model.

#### V. CONCLUSIONS

As a first attempt of applying the Faddeev equations to the  ${}^6\text{Li} + {}^3\text{He}$  breakup into three trions we find the results encouraging. The three-body model using the S-wave separable potential HS gives a surprisingly good fit to the  ${}^6\text{Li}({}^3\text{He}, {}^3\text{He}{}^3\text{He}){}^3\text{H}$  and  ${}^6\text{Li}({}^3\text{He}, t{}^3\text{He}){}^3\text{He}$  data in the region close to the symmetric QFS. The model predicts the absolute cross sections within 20–40% except for the forward angle pair (20°–20°). Also, the model correctly predicts the shape of the spectra. The spectra predicted by the model are narrower than the square of the Fourier transform of the  ${}^6\text{Li}$  cluster wave function ( ${}^3\text{H} + {}^3\text{He}$ ) partly due to strong interference effects describing the absorption inside the  ${}^6\text{Li}$  nucleus and partly due to the variation of the energy of two trions undergoing QFS. The reaction  ${}^4\text{He}(p, 2p){}^3\text{H}$  is one QF process that has been studied experimentally and in the framework of the three-body Faddeev model. At an incident energy of 100 MeV the experimental cross section at  $\theta_3 = \theta_4 = 36.7^\circ$  is about 3 times smaller than the three-body model prediction.<sup>29</sup>

The approximate inclusion of the Coulomb interaction in the three-body problem increases the calculated cross section reducing somewhat the discrepancy with the data. However, this Coulomb

effect in the breakup cross section is much smaller than in the two-body trion-trion cross section suggesting that the influence of the longer-range part of the particle-particle interaction is suppressed in the three-body breakup process.

The PWIA does not describe correctly either the absolute cross section or the shape of experimental spectra. In particular, just as in the nucleon-induced deuteron breakup, it is unable to explain the experimentally measured ratio of the QFS processes  ${}^6\text{Li}({}^3\text{He}, {}^3\text{He}{}^3\text{He}){}^3\text{H}$  vs  ${}^6\text{Li}({}^3\text{He}, t{}^3\text{He}){}^3\text{He}$ .

The fits of our admittedly simple three-body theory to the data are much better than we would have ever guessed before actually doing the calculations. In this respect two points should be especially noted. 1. Spectra shapes are well predicted even though they cover an angular range over which the fits to the relevant two-body angular distributions are poor. 2. The theory predicts the correct absolute cross section approximately, which indicates that, in the part of the phase space studied (QFS of  ${}^3\text{He}-{}^3\text{He}$  and  ${}^3\text{He}-{}^3\text{H}$ ), the  ${}^6\text{Li}$  cluster structure as  ${}^3\text{He} + {}^3\text{H}$  predominates; this we feel cannot be quite correct. Hitherto unexplored elements of three-body reaction theories, such as possible suppression of higher two-body partial waves, the role of spectroscopic factors<sup>10</sup> and of the suppressed  ${}^6\text{Li} - \alpha + d$  channel, would be very helpful in understanding our results. Further experimental studies of the  ${}^6\text{Li}({}^3\text{He}, {}^3\text{He}{}^3\text{He}){}^3\text{H}$  and  ${}^6\text{Li}({}^3\text{He}, t{}^3\text{He}){}^3\text{He}$  reactions and of other channels ( ${}^6\text{Li}({}^3\text{He}, xy)z$ ) are currently being undertaken at this laboratory.

The authors thank Dr. John McElhinney for his continued support of this project. We also thank Mr. George Miller and the cyclotron operations staff without whose help this experiment could not have been done. In addition we are deeply indebted to Mr. Eser Karaoglan and Mr. Lee Myers for contributions in many aspects of this experiment.

<sup>1</sup>L. D. Faddeev, Z. Eksp. Teor. Fiz. **39**, 1459 (1960) [Sov. Phys. JETP **12**, 1014 (1961)].

<sup>2</sup>R. D. Amado, Phys. Rev. **132**, 485 (1963); R. Aaron, R. D. Amado, and Y. Y. Yam, *ibid.* **140**, B1291 (1965);

R. Aaron and R. D. Amado, *ibid.* **150**, 857 (1966).

<sup>3</sup>E. L. Petersen, M. I. Haftel, R. G. Allas, L. A. Beach, R. O. Bondelid, P. A. Treado, J. M. Lambert, M. Jain, and J. M. Wallace, Phys. Rev. C **9**, 508

- (1974).
- <sup>4</sup>M. I. Haftel, E. L. Petersen, and J. M. Wallace, *Phys. Rev. C* **14**, 419 (1976).
- <sup>5</sup>W. Ebenhöf, *Nucl. Phys.* **A191**, 97 (1972).
- <sup>6</sup>R. C. Johnson and P. J. R. Soper, *Phys. Rev. C* **1**, 976 (1970); A. S. Reiner and A. I. Jaffe, *Phys. Rev.* **161**, 935 (1967); Gy. Bencze and P. Doleschall, *Phys. Lett.* **32B**, 539 (1970); R. Aaron and P. E. Shanley, *Phys. Rev.* **142**, 608 (1966); G. H. Rawitscher, *ibid.* **163**, 1223 (1967).
- <sup>7</sup>P. E. Shanley, *Phys. Rev.* **187**, 1328 (1969); M. S. Shah and A. N. Mitra, *Phys. Rev. C* **1**, 35 (1970); H. Hebach, P. Hennenberg, and H. Kummel, *Phys. Lett.* **24B**, 134 (1967); A. Ghovanlou and D. R. Lehman, *Phys. Rev. C* **9**, 1730 (1974).
- <sup>8</sup>B. Charnomordić, C. Fayard, and A. H. Lamot, Report No. LYCEN-76-33 (1976); *Phys. Rev.* (to be published).
- <sup>9</sup>D. S. Chuu, C. S. Han, and D. L. Lin, *Phys. Rev. C* **7**, 1329 (1973).
- <sup>10</sup>E. O. Alt, P. Grassberger, and W. Sandhas, *Nucl. Phys. B* **2**, 167 (1967); P. Grassberger and W. Sandhas, *ibid.* **B2**, 181 (1967); P. C. Tandy, E. F. Redish, and D. Bollé, *Phys. Rev. Lett.* **35**, 921 (1975); D. J. Kouri, F. S. Levin, and W. Sandhas, *Phys. Rev. C* **13**, 1825 (1976); S. K. Young and E. F. Redish, *ibid.* **10**, 498 (1974); E. F. Redish, *ibid.* **10**, 67 (1974); *Nucl. Phys.* **A225**, 16 (1974); in *Few Body Dynamics*, edited by A. N. Mitra, I. Šlaus, V. S. Bhasin, and V. K. Gupta (North-Holland, Amsterdam, 1976), p. 86; Gy. Bencze, *Nucl. Phys.* **A210**, 568 (1973); D. J. Kouri and F. S. Levin, *Phys. Rev. A* **10**, 1616 (1974); *Nucl. Phys.* **A250**, 127 (1975).
- <sup>11</sup>I. Šlaus, in *Few Body Dynamics* (see Ref. 10), p. 584.
- <sup>12</sup>D. Vranić and I. Šlaus, *Fizika* **8**, 155 (1976).
- <sup>13</sup>G. R. Plattner, M. Bornand, and K. Alder, *Phys. Lett.* **61B**, 21 (1976); A. S. Rinat, L. P. Kok, and M. Stingl, *Nucl. Phys.* **A190**, 328 (1972); T. K. Lim, *Phys. Lett.* **56B**, 321 (1975).
- <sup>14</sup>A. K. Jain, J. Y. Grossiord, M. Chevallier, P. Gaillard, A. Guichard, M. Gusakow, and J. R. Pizzi, *Nucl. Phys.* **A190**, 328 (1972).
- <sup>15</sup>J. V. Noble, *Phys. Lett.* **55B**, 433 (1975).
- <sup>16</sup>Y. M. Shin, D. M. Skopik, and J. J. Murphy, *Phys. Lett.* **55B**, 297 (1975), and references therein.
- <sup>17</sup>D. R. Thompson and Y. C. Tang, *Nucl. Phys.* **A106**, 591 (1968); A. M. Young, S. L. Blatt, and R. G. Seyler, *Phys. Rev. Lett.* **25**, 1764 (1970).
- <sup>18</sup>H. Orihara, M. Baba, M. Akyamas, S. Iwasaki, T. Nakagawa, H. Veno, and M. Watanabe, *J. Phys. Soc. Japan* **29**, 533 (1970); P. D. Forsyth and R. R. Perry, *Nucl. Phys.* **67**, 517 (1965); A. R. Knudson and E. A. Wolicki, in *Proceedings of the Conference on Direct Interactions and Nuclear Reaction Mechanisms, Padua, 1962* (Gordon and Breach, New York, 1963), p. 981; F. C. Young, P. D. Forsyth, and J. B. Marion, *Nucl. Phys.* **A91**, 209 (1967).
- <sup>19</sup>J. M. Lambert, R. J. Kane, P. A. Treado, L. A. Beach, E. L. Peterson, and R. B. Theus, *Phys. Rev. C* **4**, 2010 (1971).
- <sup>20</sup>P. G. Roos, D. A. Goldberg, N. S. Chant, R. Woody, III, and W. Reichert, *Nucl. Phys.* **A257**, 317 (1976); D. Bachelier, M. Bernas, C. Detraz, P. Radvanyi, and M. Roy, *Phys. Lett.* **26B**, 283 (1968).
- <sup>21</sup>I. V. Kurdynov, V. G. Neudatchin, and Yu. F. Smirnov, *Phys. Lett.* **31B**, 426 (1970).
- <sup>22</sup>E. L. Petersen, R. G. Allas, R. O. Bondelid, A. G. Pieper, and R. B. Theus, *Phys. Lett.* **31B**, 209 (1970); E. L. Petersen, R. G. Allas, R. O. Bondelid, D. I. Bonbright, A. G. Pieper, and R. B. Theus, *Phys. Rev. Lett.* **27**, 1454 (1971).
- <sup>23</sup>I. Šlaus, R. G. Allas, L. A. Beach, R. O. Bondelid, E. L. Petersen, J. M. Lambert, P. A. Treado, and R. A. Moyle, *Nucl. Phys.* (to be published).
- <sup>24</sup>J. Bruinsma, W. Ebenhöf, J. H. Stuivenberg, and R. van Wageningen, *Nucl. Phys.* **A228**, 52 (1974).
- <sup>25</sup>Z. Bajzer, (a) *Nuovo Cimento* **A22**, 300 (1974); and (b) *Z. Physik* **A278**, 97 (1976).
- <sup>26</sup>To obtain our Eq. (12) for half-shell scattering we rederive Eq. (17) of Ref. 25(b) for quasi-two-body states  $|kE\rangle$  where for off-shell scattering  $E \neq k^2$ . Following Eqs. (1)–(17) here, except with  $H_0|kE\rangle = E|kE\rangle$  we obtain for Eq. (17) (with  $E = k^2$ )
- $$\begin{aligned} \langle kE|S|k'E'\rangle = & -2\pi i\delta(E-E') \exp\{-\pi/2[\eta(k)+\eta(k')]\} \\ & \times [\Gamma \times (1-i\eta(k)) \Gamma(1-i\eta(k'))]^{-1} \\ & \times (2k^2)^{2i\eta(k)} (2k'^2)^{2i\eta(k')} T_0(k, k'; k^2+i0), \end{aligned}$$
- where  $T_0(k, k'; k^2+i0)$  is given by Eq. (26) of Ref. 25(b). The quantity multiplying  $-2\pi i\delta(E-E')$  is identified as the (half-off-shell) scattering amplitude. Whereas H. van Haeringen and R. van Wageningen [*J. Math. Phys.* **16**, 1441 (1975)] point out that the full Coulomb  $T$  matrix is undefined as a function, the quantity involved here  $T_0(k, k'; k^2+i0)$  is well defined [see for example Ref. 25(b)].
- <sup>27</sup>E. O. Alt, in *Few Body Dynamics* (see Ref. 10), p. 76.
- <sup>28</sup>E. O. Alt, W. Sandhas, H. Zankel, and H. Ziegelmann, *Phys. Rev. Lett.* **37**, 1537 (1976).
- <sup>29</sup>S. K. Young and E. F. Redish, *Phys. Rev. C* **10**, 498 (1974).